The siderophore-interacting protein YqjH acts as a ferric reductase in different iron assimilation pathways of *Escherichia coli*

Marcus Miethke,* Jie Hou and Mohamed A. Marahiel

Department of Chemistry/Biochemistry, Hans Meerwein Strasse, Philipps University Marburg, D-35032 Marburg, Germany

- Supporting Material -

A

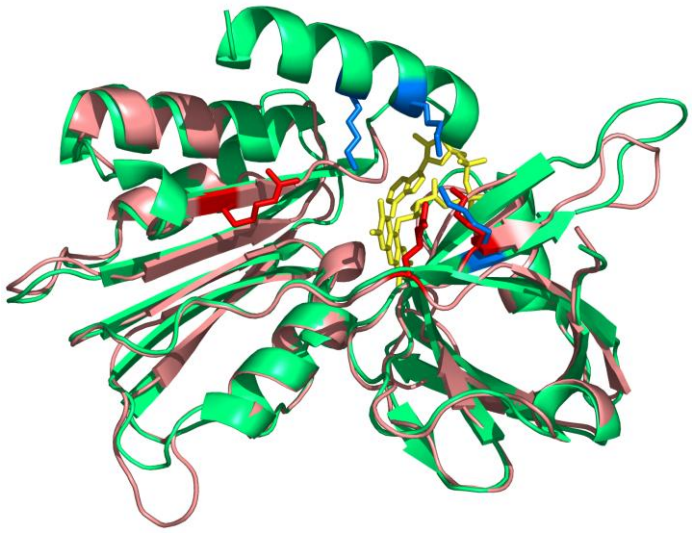

B

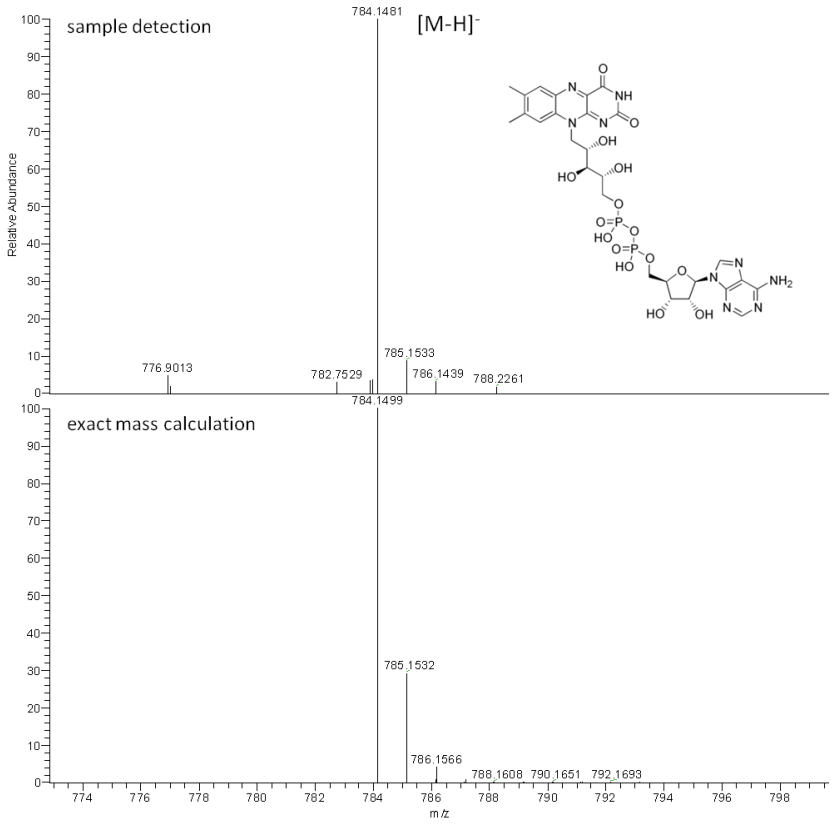

Fig. S1: (A) Structural model of *E. coli* YqjH (salmon red) and ViuB from *S. putrefaciens* (in green with FAD cofactor in yellow) according to Fig. 1B, but with minimized RMSD between aligned residues (calculated with PyMOL software version 0.98). Conserved basic residues associated with substrate binding are indicated in red (YqjH) or in blue (ViuB). **(B)** Detection of released FAD cofactor by FTICR-MS in the negative mode after holo-protein denaturation and removal of the protein fraction. 100 µg of holo-YqjH were desalted and then treated with 90 % methanol in water prior to HPLC and mass analysis. The upper spectrum shows the detected mass, the lower spectrum shows the calculation of the exact mass of $[FAD\text{-}H]^-$.

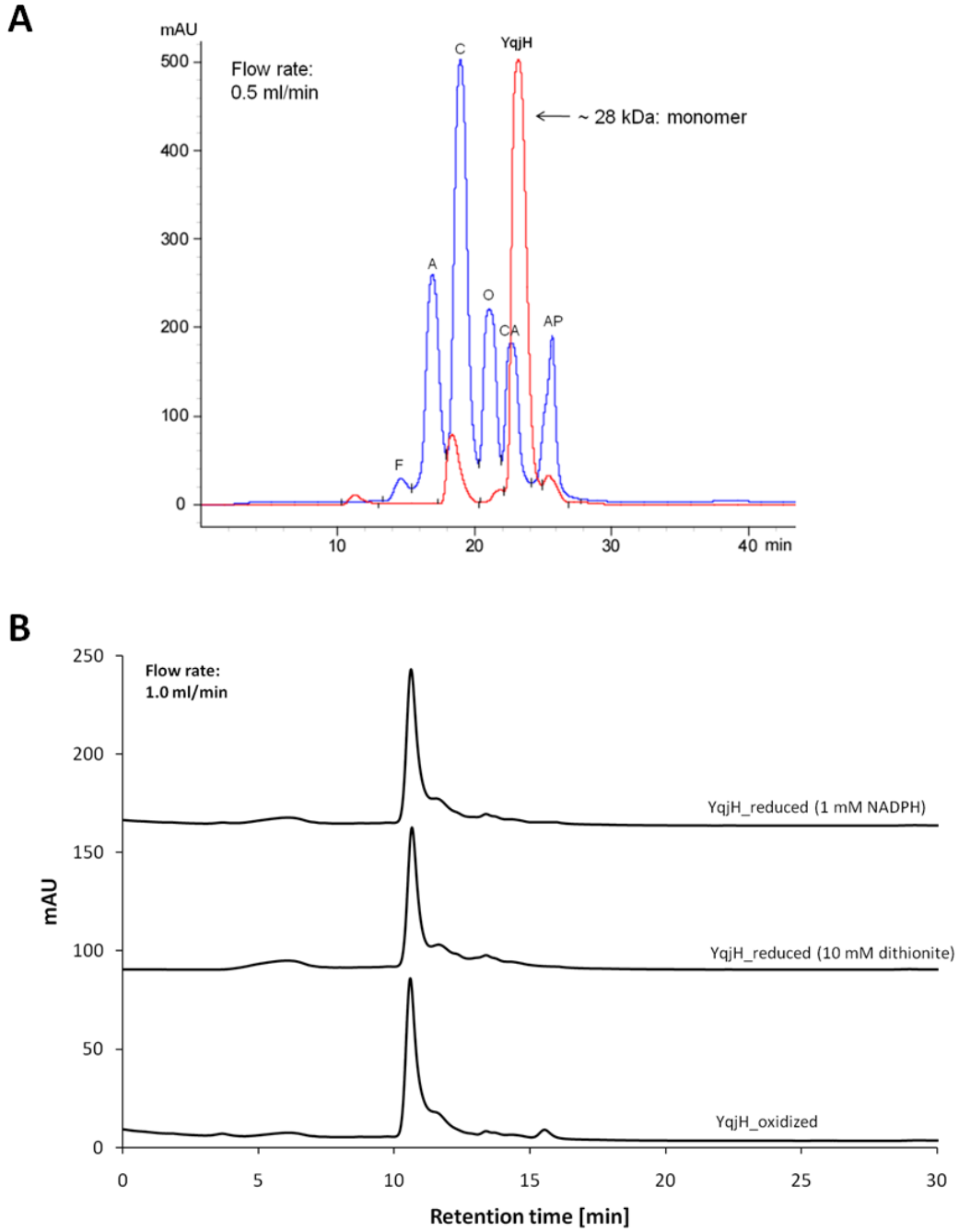

Fig. S2: Analytical gel filtration with recombinant YqjH. **(A)** Retention time profile of YqjH (red line) together with an analytical protein calibration standard (blue line) containing Ferritin, F; Aldolase, A; Conalbumin, C; Ovalbumin, O; Carbonic Anhydrase, CA; Aprotinin AP. **(B)** Gel filtration profiles obtained under anaerobic conditions with 10 µg of oxidized YqjH, 10 µg of dithionite-reduced YqjH, 10 µg of NADPH-reduced YqjH.

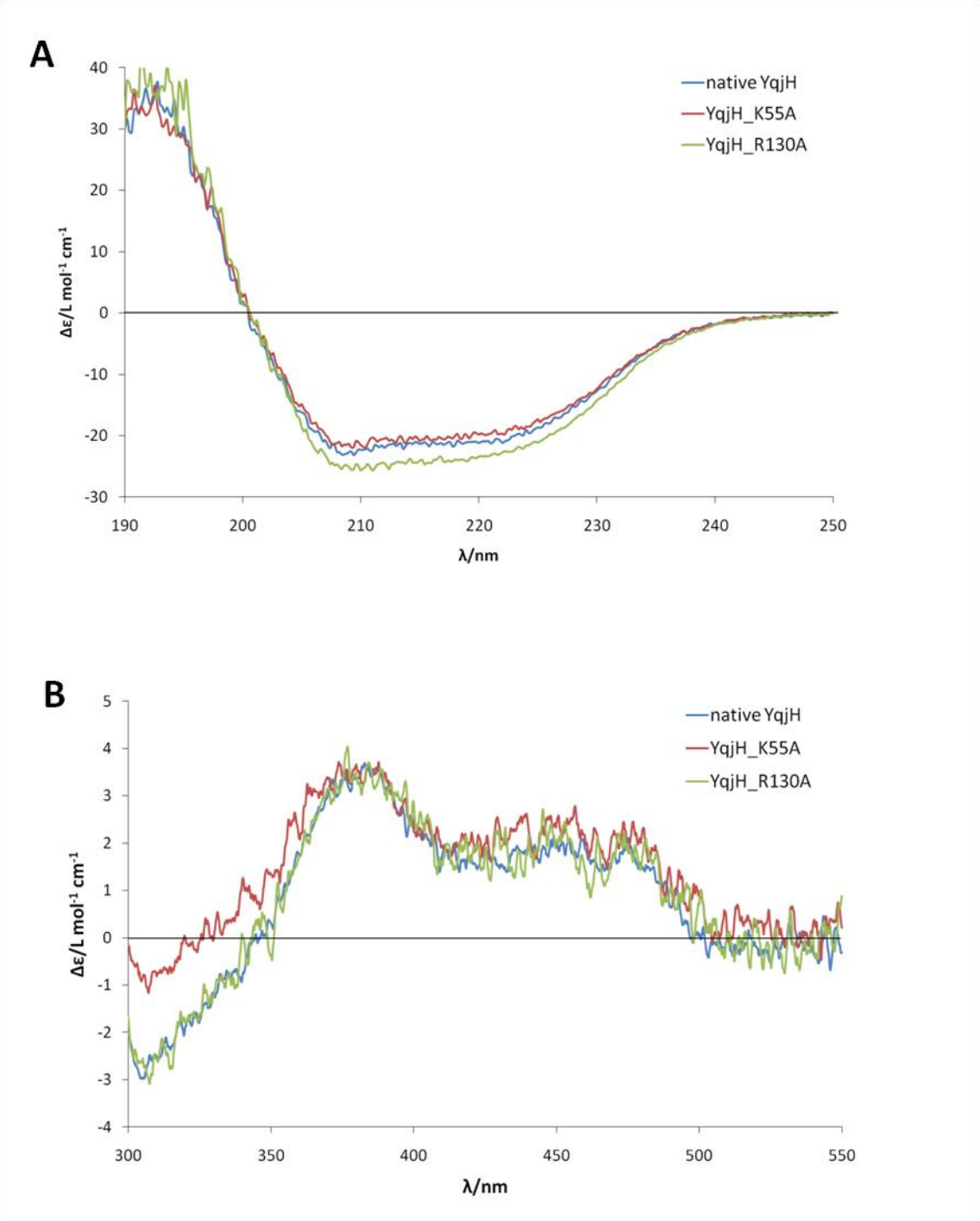

Fig. S3: CD spectroscopy with native YqjH and alanine substituted variants YqjH_K55A and YqjH_R130A in far and near UV regions at 20 °C. **(A)** Scans in far UV region from 250 to 190 nm. Solutions of 4 µM protein in 1 mM Tris-HCl pH 8.5 were measured in a 0.1 cm path length cuvette. **(B)** Scans in near UV/vis region from 550 to 300 nm. Solutions of 45 µM protein in 5 mM Tris-HCl pH 8.5 were measured in a 0.5 cm path length cuvette. All scans are results of 5 cycles of data accumulation.

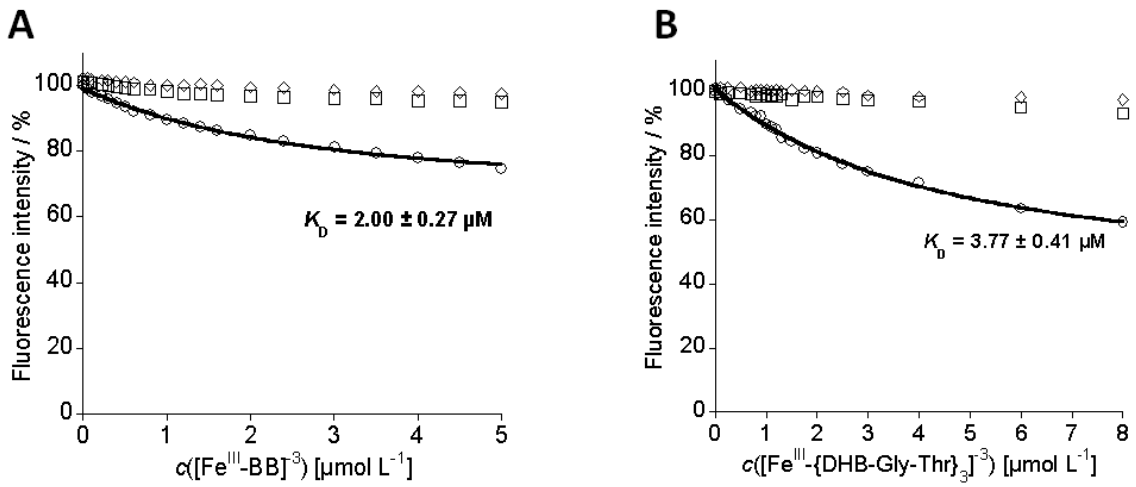

Fig. S4: Fluorescence titrations with native YqjH and YqjH_K55A and YqjH_R130A derivatives. For analysis, 1.0 µM of each protein (YqjH, circles; YqjH_K55A, rectangles; YqjH_R130A, diamonds) were titrated with **(A)** ferric bacillibactin ($[Fe^{III}\text{-}BB]^{-3}$) or **(B)** the ferric (2,3-dihydroxybenzoyl-glycine-threonine)$_3$ complex ($[Fe^{III}\text{-}\{DHB\text{-}Gly\text{-}Thr\}_3]^{-3}$), respectively. In cases of observed fluorescence quenching, fittings according to the Law of Mass Action were performed (assuming 1:1 binding stoichiometries), and dissociation constants (K_D values) were calculated.

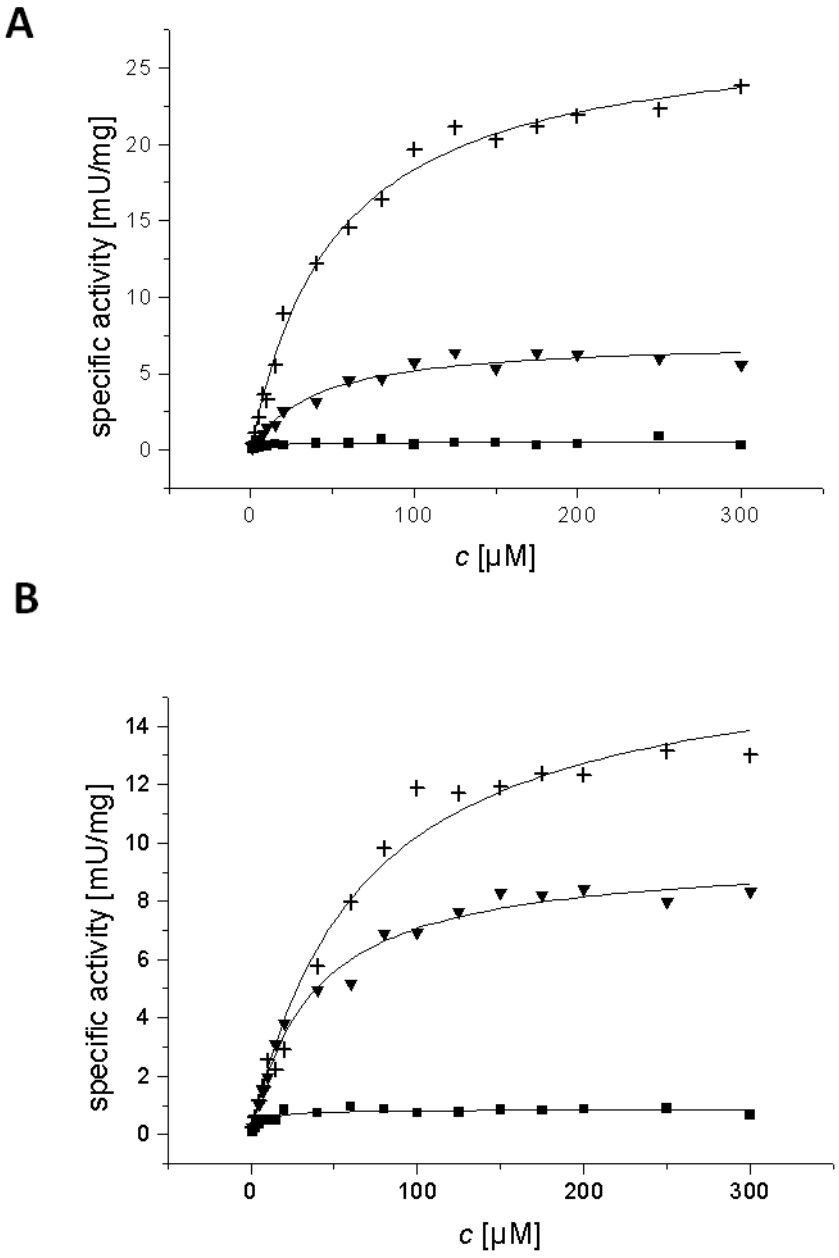

Fig. S5: Kinetics with alanine-substituted derivatives YqjH_K55A **(A)** and YqjH_R130A **(B)**. Ferric substrate dependent kinetics were carried out with 2 mM NADPH, 2 µM YqjH and varied concentrations of ferric enterobactin (squares), ferric (2,3-dihydroxybenzoylserine)$_3$ (triangles down), and ferric dicitrate (crosses). Kinetic parameters obtained after fitting according to the Michaelis-Menten type model are given in Table 1.

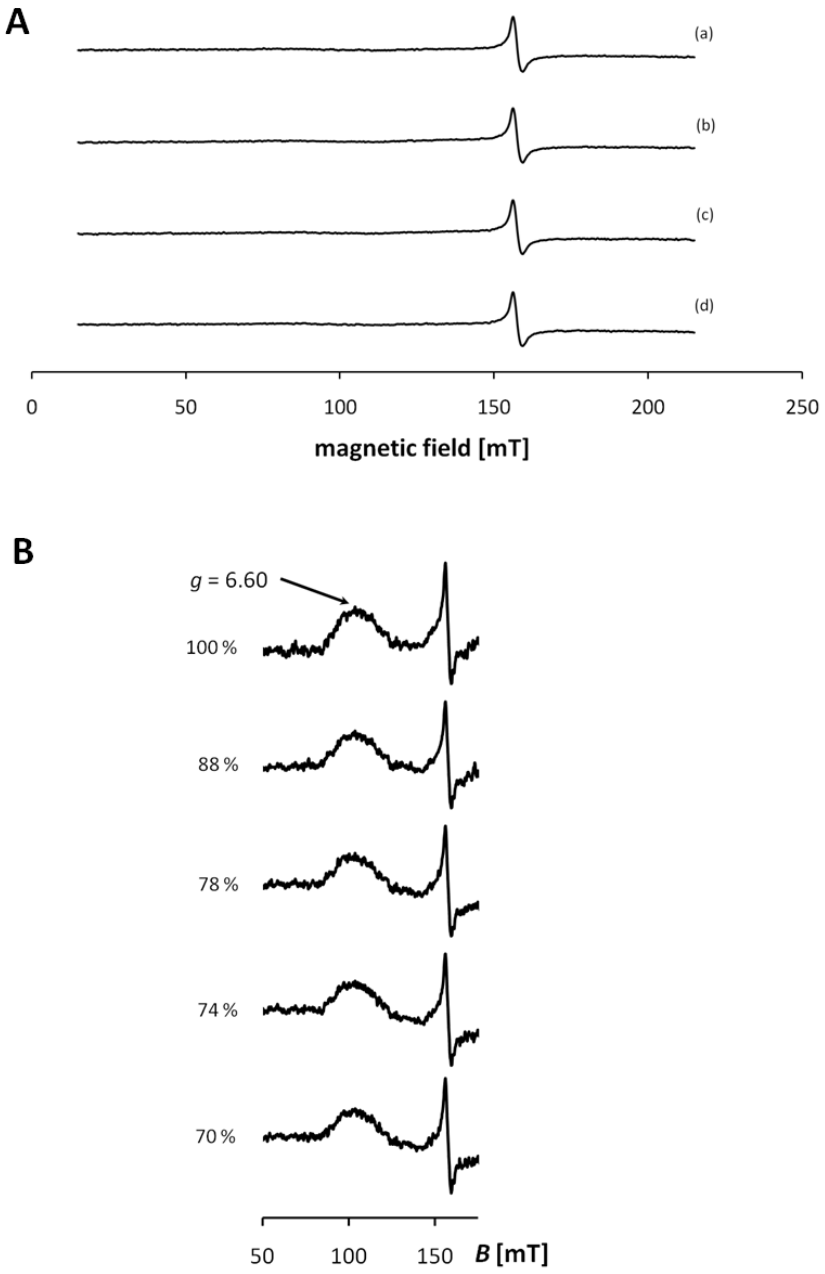

Fig. S6: EPR redox titrations with free ferric enterobactin and ferric enterobactin in complex with 5-deaza-5-carba-FAD-reconstituted YqjH. **(A)** Titration with free ferric enterobactin (30 µM) at pH 8.5 without addition of dithionite (a), after addition of 0.5 mM dithionite (b), after addition of 2.5 mM dithionite (c), after addition of 25 mM dithionite (d). **(B)** Titration with 30 µM ferric enterobactin in presence of 75 µM 5-deaza-5-carba-YqjH at pH 8.5. Shown are representative spectra together with the determined percentage changes of the amplitude of the *g* = 6.60 signal.